JPE 9-6-3

Radial Force Control of a Novel Hybrid Pole BLSRM

Huijun Wang*, Dong-Hee Lee*, and Jin-Woo Ahn†

†*Dept. of Electrical and Mechatronics Engineering., Kyungsung University, Busan, Korea

ABSTRACT

This paper presents a novel hybrid pole BLSRM (Bearingless Switched Reluctance Motor) and its radial force control scheme. The proposed hybrid pole BLSRM has separated radial force poles and rotating torque poles. According to the FEM analysis, the proposed BLSRM has an excellent linear characteristic of radial force and controllability that is independent from the torque current. The radial force can be produced by the radial force winding which is wound at the separated radial force poles. The rotating torque is produced by the excitation current of the torque windings which are wound at the torque pole. The proposed radial force control scheme is independent of the phase torque winding current. A simple PID controller and look-up table are used to maintain a constant rotor air-gap. The proposed BLSRM and its radial force control scheme are verified by FEM analysis and experimental tests.

Keywords: Bearingless, Switched Reluctance Motor, Radial force, Suspending force

1. Introduction

In an effort to solve some of the difficulties of traditional mechanical bearings for high speed machines and environmental problems, non-mechanical suspension technologies have recently become the subject of many studies[1]. Air and magnetic bearing system can provide excellent suspension performance for rotating machines. But, the additional equipment requires a complex control system and additional costs. Furthermore, motor size is greatly increased when installing additional air or magnetic bearings. Bearingless motors are introduced to overcome these problems. The suspension force of bearingless motors is produced by the additional winding current and the rotor flux without any outer mechanical bearing systems[1-4].

SRMs (switched reluctance motor) have inherent radial force from the interaction of the stator and the rotor poles[5-11]. As a result, SRMs have a high potential for use in bearingless drives[3-4]. Conventional BLSRMs are made by using the conventional structure of SRMs. Only the additional windings for the suspending forces are wound to the stator poles. So, conventional BLSRMs have separated phase torque winding and suspending winding in the stator poles[2-4]. The radial force of conventional BLSRMs is coupled to the rotational torque and the suspending force and as a result the control of the radial force is very difficult.

This paper presents a novel hybrid pole BLSRM and its radial force control scheme. The proposed motor has separated stator poles for radial force winding and phase winding. The radial force stator poles are placed opposite and in a perpendicular position for continuous radial force generation. In order to keep the rotor to the center of the

Manuscript received Dec. 30, 2009; revised Aug. 28, 2009
†Corresponding Author: jwahn@ks.ac.kr
Tel: +82-51-663-4773, Fax: +82-51-624-5980, Kyungsung Univ.
*Dept. of Electrical and Mechatronics Eng., Kyungsung Univ.

motor, the radial forces in the x and y directions are controlled by the radial force winding currents. The proposed radial force control scheme is independent of the phase torque winding current. A simple PID controller and a look-up table are used to maintain a constant rotor air-gap.

The proposed BLSRM and its radial force control scheme are verified by FEM analysis, simulation and experimental tests.

2. The Proposed Hybrid Pole BLSRM

2.1 Conventional BLSRM

Fig. 1 shows the basic structure and torque-radial force characteristics of a conventional double winding BLSRM. As shown in Fig. 1(a), the rotor and stator are the same as a 12/8 pole SRM. However, a conventional BLSRM has an additional suspending winding at each stator pole. The phase winding is series connected to each stator phase pole, and the suspending windings are connected symmetrically as shown in Fig. 1(a). As a result, conventional 12/8 pole BLSRMs have 3-phase windings and 6 suspending windings. The 3-phase windings are connected to an asymmetric converter to control the phase currents. The 6 suspending windings are connected to an H-bridge converter to control the suspending currents. The suspending winding current produces linkage flux to control the air-gap of the rotor.

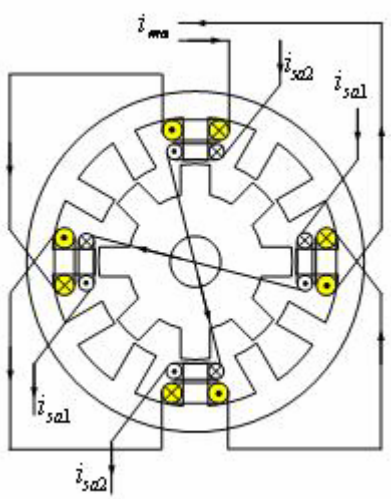

(a) Torque and suspending windings of a conventional BLSRM

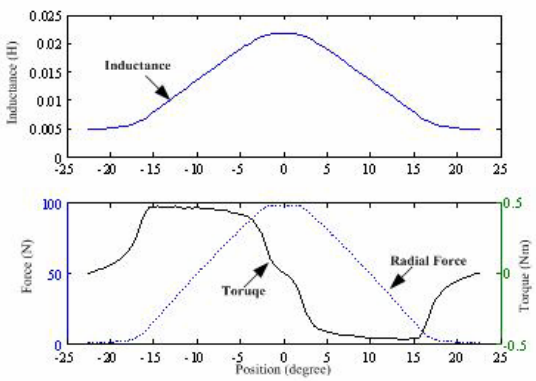

(b) Phase torque and radial force of a conventional BLSRM

Fig. 1. Basic structure and torque characteristics of a conventional BLSRM.

Fig. 1(b) shows the torque and radial force profile of the conventional BLSRM corresponding to Fig. 1(a). As shown in Fig. 1(b), the phase torque and radial force are repeated at the same stator pole. For continuous radial force control, the torque region of each phase should be restricted. As a result, the total torque has a larger torque dip than conventional SRMs. Furthermore, the radial force is generated by the current of the torque winding.

During the conduction period of phase A (-15deg ~ 15deg), the radial forces from suspending windings a1 and a2 are derived as follows [1-3]:

$$\begin{bmatrix} F_{a1} \\ F_{a2} \end{bmatrix} = \begin{bmatrix} F_x \\ F_y \end{bmatrix} = 4 \cdot K_f(\theta) \cdot N_m \cdot i_{ma} \cdot N_s \cdot \begin{bmatrix} i_{sa1} \\ i_{sa2} \end{bmatrix} \quad (1)$$

where, $K_f(\theta)$ is a function of the rotor angular position θ and the dimensions of the motor. N_m and N_s are the turn numbers of the torque and the suspending windings, respectively. In (1), the current i_{ma} of the torque winding of phase A is related to radial force generation. If the torque current is changed, the radial force is varied by this coupling factor.

2.2 The proposed BLSRM

Fig. 2 shows the structure of the proposed BLSRM. The proposed motor has 8 stator poles and 10 rotor poles. The rotor pole's arcs are the same, but stator poles are designed as hybrid pole structures. In Fig. 2, *x1*, *x2*, *y1* and *y2* in the wide stator poles are for suspending windings,

and *ma* and *mb* in the conventional stator poles are for phase windings. As shown in Fig. 2, the suspending windings and torque windings are in separate positions. So, the proposed BLSRM requires one 2-phase converter and four H-bridge converters for radial force control. It also uses six fewer switching power devices and six fewer power diodes than conventional BLSRMs.

Radial force is controlled by the symmetrically positioned winding currents of the suspending poles. The y1 and y2 winding currents can move the rotor position in the y-direction, and the x1 and x2 winding currents can move the rotor position in the x-direction. The radial force from the suspending windings is almost constant at any rotor position, and the constant radial force can suspend the rotor in a constant air-gap. In a conventional BLSRM, the radial force can be changed according to the rotor position. As a result, constant radial force control is very difficult.

The torque poles are designed for continuous phase torque generation, and the torque characteristic of the proposed BLSRM is similar to conventional SRMs.

Fig. 3 shows the magnetic flux path of the suspending stator pole and the rotor pole according to rotor position. In Fig. 3, β_r is the rotor pole arc, and τ_r denotes the rotor pole pitch. β_{ss} is the pole arc of the suspending stator pole, and β_0 is defined as half of $\tau_r - \beta_r$. The air gap of the stator pole and the rotor pole are defined as l_a. In Fig. 3(a), the suspending stator pole is aligned as one rotor pole and in Fig. 3(b) it is aligned as two rotor poles.

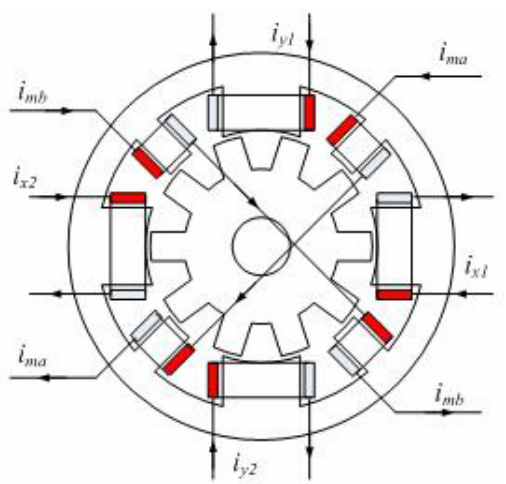

Fig. 2. Proposed hybrid pole BLSRM.

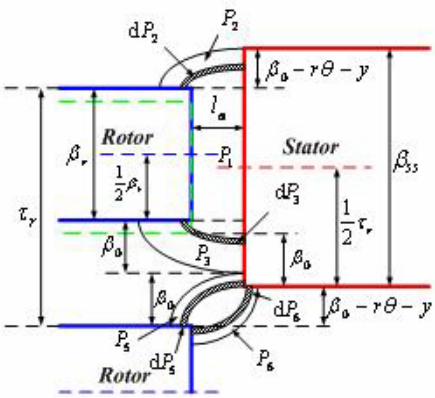

(a) One rotor pole is aligned

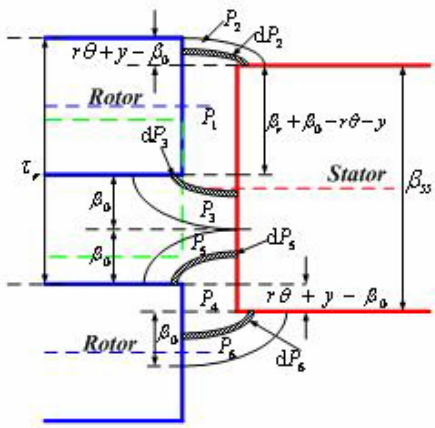

(b) Two rotor poles are aligned

Fig. 3. Simplified equivalent magnetic circuit of air-gap according to rotor position.

The suspending pole arc β_{ss} is designed as τ_r which is the rotor pole pitch. As a result, the suspending pole is always aligned by one rotor pole arc β_r to produce a constant radial force.

We assume that r is the rotor radius in Fig. 3 and that *x* and *y* are moving in the x-direction and the y-direction, respectively.

The permence can be calculated in the case of Fig. 3(a) as follows:

$$P_{x1} = \frac{\mu_0 l \beta_r}{l_0 - x + \frac{y\theta}{2}} + 3\frac{\mu_0 l}{a\pi - 2}\left[a \cdot \ln\frac{al_a + \beta_0}{al_a} + \frac{a\pi - 4}{\pi} \cdot \ln\frac{2l_a + \pi\beta_0}{2l_a}\right] \quad (2)$$
$$-\frac{\mu_0 l}{a\pi - 2}\left[a \cdot \ln\frac{al_a - r\theta - y - \beta_0}{al_a} + \frac{a\pi - 4}{\pi} \cdot \ln\frac{2l_a + \pi(-r\theta - y + \beta_0)}{2l_a}\right]$$

And the case of Fig. 3(b) can be derived as follows:

$$P_{x1}=\frac{\mu_0 l\beta_r}{l_0-x+\frac{y\theta}{2}}+3\frac{\mu_0 l}{a\pi-2}\left[a\cdot\ln\frac{al_a+\beta_0}{al_a}+\frac{a\pi-4}{\pi}\cdot\ln\frac{2l_a+\pi\beta_0}{2l_a}\right] \quad (3)$$
$$-\frac{\mu_0 l}{a\pi-2}\left[a\cdot\ln\frac{al_a+r\theta+y-\beta_0}{al_a}+\frac{a\pi-4}{\pi}\cdot\ln\frac{2l_a+\pi(r\theta+y-\beta_0)}{2l_a}\right]$$

where, l is the axial length of the stator and the rotor core, μ_0 is free permeability, l_0 is the air-gap when the rotor is positioned in the center position, and α is the coefficient for the FEM analysis.

The suspending radial force at the *x1* winding stator pole can be derived from the permeance as follows:

$$F_x=\frac{\partial W_{x1}}{\partial x}=\frac{1}{2}\cdot\frac{\partial P_{x1}}{\partial x}\left(N_{x1}\cdot i_{x1}\right)^2 \quad (4)$$

$$F_y=\frac{\partial W_{x1}}{\partial y}=\frac{1}{2}\cdot\frac{\partial P_{x1}}{\partial y}\left(N_{x1}\cdot i_{x1}\right)^2 \quad (5)$$

where, N_{x1} and i_{x1} are the turn numbers of the suspending winding of the *x1* pole and the winding current, respectively.

In order to get excellent control performance from the BLSRM, decoupling of the radial force and the torque are very important. Also the radial force of the x- and y-direction should be separated.

Fig. 4 and Fig. 5 show the radial force and output torque from the suspending force winding current and the rotor position. The suspending winding current i_{x1} is concerned with the x-direction radial force. As shown in Fig. 4 and Fig. 5, the radial force in the x-direction is much concerned with the suspending winding current i_{x1}. However, the force in the y-direction and the output torque are very low. As a result, the radial force in the x-direction can be controlled by the currents i_{x1} and i_{x2} in the radial force windings of the *x1* and *x2* stator poles, respectively. Similarly, the radial force in the y-direction can be controlled by the currents of the radial force windings of the *y1* and *y2* poles. As a result, each direction radial force can be controlled independently.

3. Radial Force Control

In order to suspend the rotor and keep a constant air-gap,

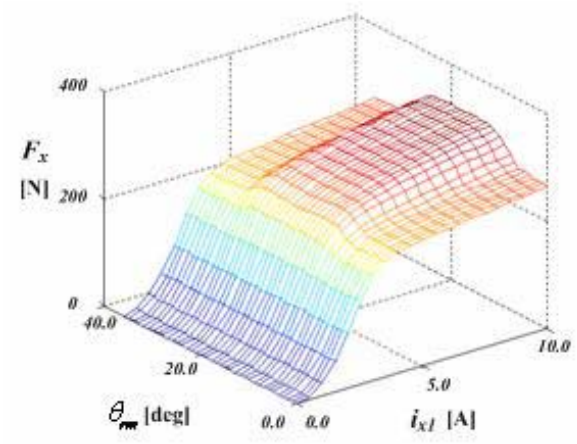

(a) Radial force in x-direction

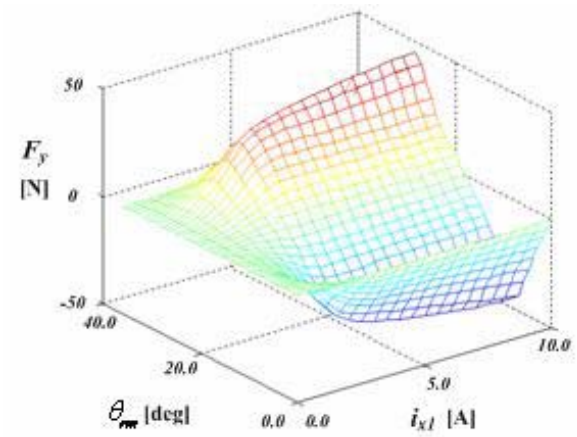

(b) Radial force in y-direction

Fig. 4. FEM analysis results of radial force according rotor position and current of x1 stator pole.

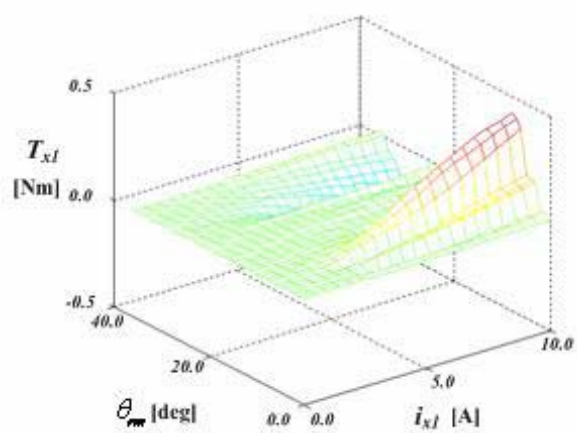

Fig. 5. Output torque of radial force winding current and rotor position.

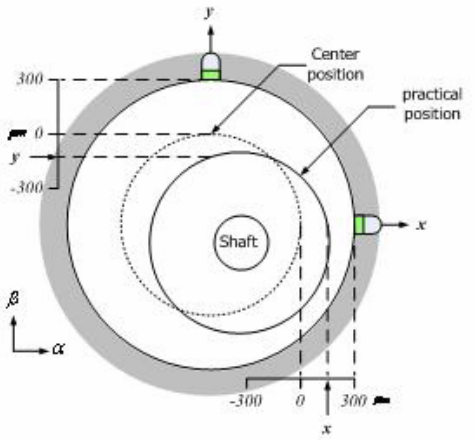

Fig. 6. Air-gap displacement according to rotor eccentricity.

radial force control is very important. The air-gap of the rotor can be detected by air-gap sensors which are attached in the α and β directions. From the gap sensor, rotor displacement form the center position can be detected.

Fig. 6 shows air-gap displacement according to rotor eccentricity. As shown in Fig. 6, the output of the air-gap sensor is zero at the center position, and the output signals are changed according to the air-gap displacement in the x and y-directions.

Fig. 7 shows the windings of the proposed hybrid pole BLSRM and the asymmetric converter for radial force control in the *x2* winding pole. As shown in Fig. 7(a), each suspending winding pole is connected to the asymmetric converter to bear the rotor position.

Fig. 8 shows the radial force control scheme for a constant air-gap. In order to make the suspending winding current references, very complex calculations are required in conventional BLSRMs.

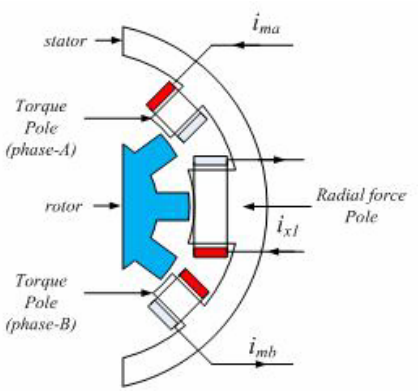

(a) Windings of hybrid pole BLSRM

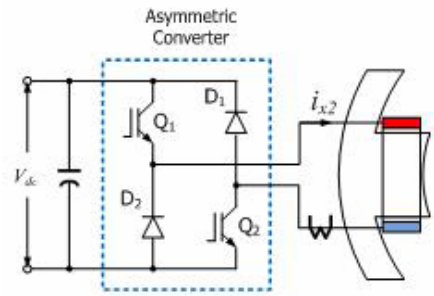

(b) Asymmetric converter for radial force control

Fig. 7. Structure and converter connection of the proposed BLSRM.

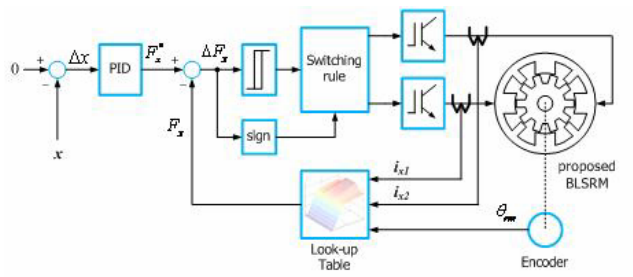

Fig. 8. Radial force control scheme using look-up table and PID controller.

The reference of the radial force can be obtained as follows:

$$F_x^* = K_P \cdot \Delta x + K_I \cdot \int \Delta x \cdot dt + K_D \cdot \frac{d\Delta x}{dt}$$
$$F_y^* = K_P \cdot \Delta y + K_I \cdot \int \Delta y \cdot dt + K_D \cdot \frac{d\Delta y}{dt} \quad (6)$$

The practical radial force can be calculated by the following look-up table:

$$F_x = f_x(i_{x1}, \theta_{rm}) + f_x(i_{x2}, \theta_{rm}) \quad (7)$$

The non-linear function f_x is designed as a look-up table for radial force calculation. The look-up data is stored in the internal memory of the DSP.

Fig. 9 shows the switching rules for the radial force control of x-direction converters. Each asymmetric converter is placed in an opposite position. As a result, the switching signals are opposite. If the switching state of converter x1 is '1', then a positive radial force in the x-direction is produced and the switching state of converter x2 is '-1'.

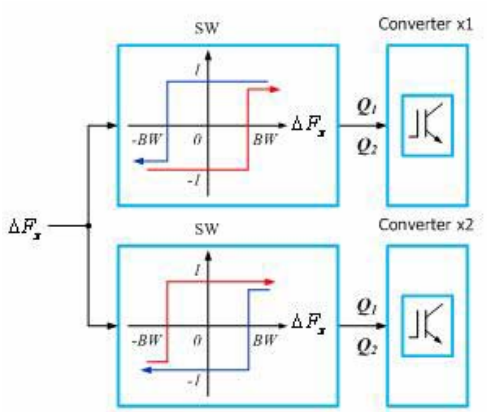

Fig. 9. Switching rules for radial force control of x-direction converters.

4. Simulation and Experimental Results

Table 1 shows the specifications of the hybrid BLSRM.

Table 1. The specifications of the hybrid BLSRM.

Parameter	Value
Number of Stator Poles	8
Number of Rotor Poles	10
Pole arc of stator for torque [deg]	18
Pole arc of stator for radial force [deg]	36
Pole arc of rotor [deg]	18
Length of axial stack [mm]	40
Outer Diameter of Stator [mm]	112
Inner Diameter of Stator [mm]	62
Yoke Thickness of Stator [mm]	10
Length of Air Gap [mm]	0.3
Inner Diameter of Rotor [mm]	18
Yoke Thickness of Rotor [mm]	9.7

Fig. 10, 11 and 12 show the simulation results of the prototype motor and the radial force control scheme. Fig. 10 shows the radial force in the x and y directions and the suspending winding currents. In order to bear the rotor in the center position, the radial forces are controlled by the suspending winding currents regardless of motor speed and torque. In the simulation, a 10[N] load is applied to the rotor shaft in the y-direction. Fig. 11 shows the air-gap trajectory. The rotor position is moved to the center position according to the radial force control. As a result, the rotor can keep a constant air-gap for smooth rotation.

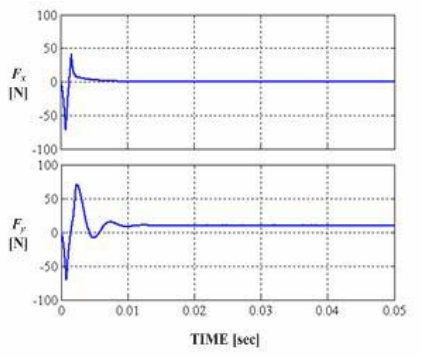

(a) Radial force

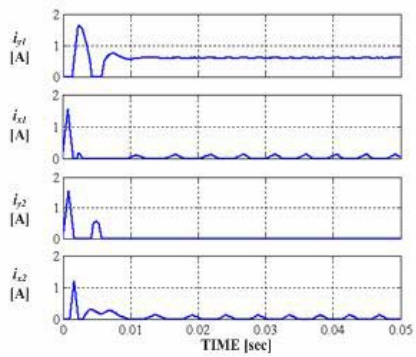

(b) Suspending winding currents

Fig. 10. Radial force and suspending winding currents.

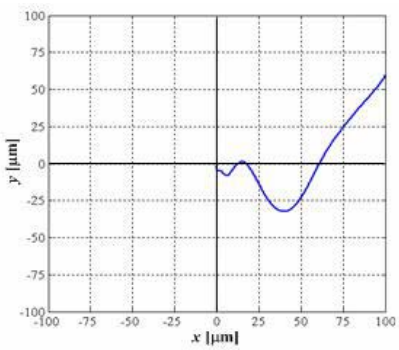

Fig. 11. Air-gap displacements of the BLSRM.

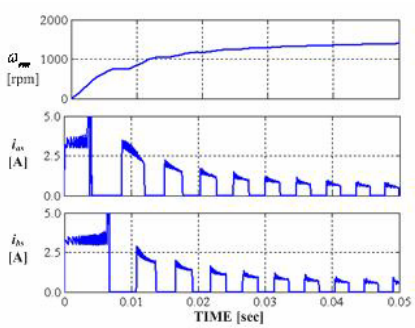

Fig. 12. Speed and phase windings current.

Fig. 12 shows the motor speed and phase winding currents. The phase winding currents produce the motor torque, and the torque is controlled to keep the motor speed.

To verify the proposed control scheme, a digital controller using a DSP by TI (Texas Instruments) is designed[12]. The suspending winding currents are measured by current sensors, and the signals are connected to a 12bit AD converter embedded DSP. Internal flash memory is used for making the look-up table of the radial force. The look-up table is made every 0.1 [deg.] and 0.1[A] steps. The linear interpolation method is used for detail radial force calculation.

Fig. 13 shows the prototype BLSRM and the experimental configuration. A weight load is directly applied to the shaft to give a disturbance.

Fig. 14 shows the radial forces in the x-y directions and the air-gap displacements at the stop position. The rotor shaft is located in a temporary position. The x and y direction winding currents produce a radial force to suspend the rotor shaft, and the shaft position is moved to the center position as shown in Fig. 14. The shaft load is 2.5 and 5[N] in the x and y directions, respectively.

(a) Stator

(b) Rotor

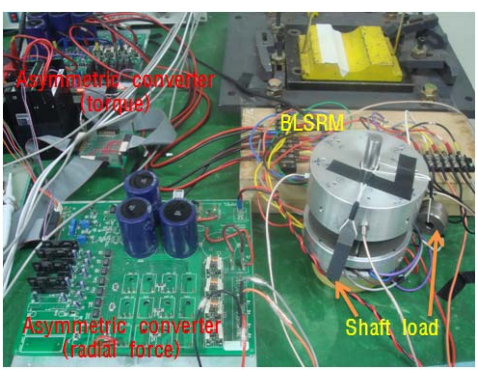

(c) Experimental configuration

Fig. 13. Prototype BLSRM and experimental configuration.

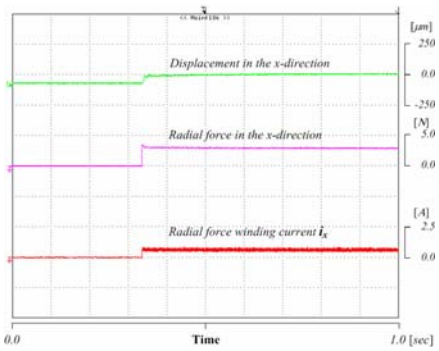

(a) x-direction

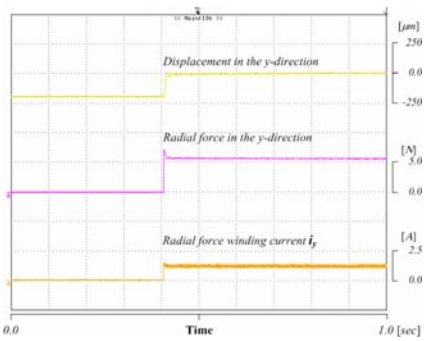

(b) y-direction

Fig. 14. Radial force and air-gap displacement at static condition.

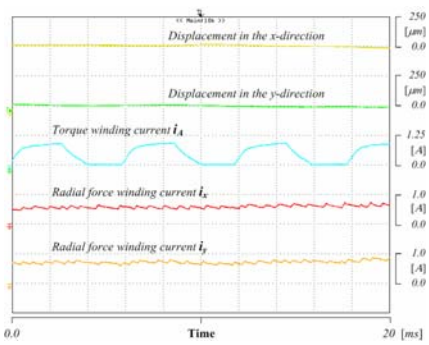

(a) At 1,000[rpm]

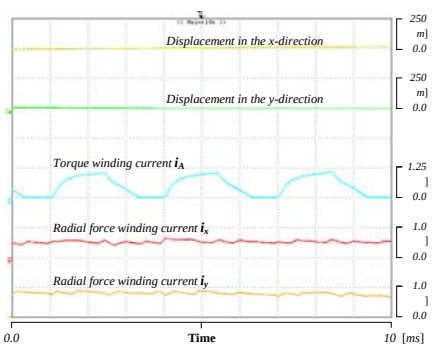

(b) At 2,000[rpm]

Fig. 15. Radial force and air-gap displacement at rotating condition.

Fig. 15 shows the air-gap displacements and winding currents when the motor speed is 1,000 and 2,000[rpm], respectively. The waveform of the torque winding current is the same as conventional two-phases SRMs. The radial force winding currents are controlled to maintain the shaft position in the center. As shown in Fig. 15, the rotor shaft can keep the center position when the rotating conditions are met.

Fig. 16 and Fig. 17 show the air-gap displacements and the winding currents when the shaft-load and the speed conditions change, respectively. In the Fig. 16, the shaft load in the y-direction is changed from 4 to 6[N]. The suspending current in the y-direction is increased to bear the increased shaft load. The air-gap can maintain the center position and rotation is very stable. In Fig. 17, the motor speed is changed from 2,000 to 1,000[rpm]. According to the changing speed, the torque winding current is changed to control the motor speed. But the air-gap displacements can keep the center position without any vibration.

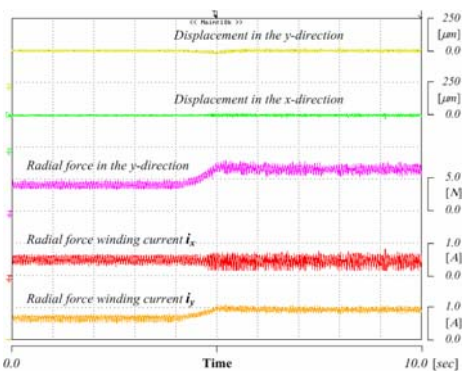

Fig.16. Experimental result in shaft-load variation(1,000[rpm]).

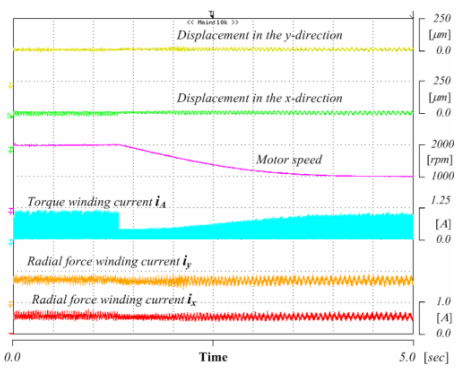

Fig. 17. Experimental result in motor speed variation.

5. Conclusions

This paper presents a novel hybrid stator pole BLSRM and its radial force control scheme. The proposed hybrid pole BLSRM has separated torque and suspending winding poles. Each pole winding currents is concerned with torque and radial force production, respectively.

A simple radial force controller using a PID controller and a look-up table is used to maintain a constant air-gap. Because the radial force is decoupled from the torque current, the torque winding currents are not considered to control the air-gap. In the proposed BLSRM and control scheme, the air-gap can keep the center position under the unloaded and loaded conditions in both the simulation and the experimental results.

Acknowledgment

This work is the outcome of a Manpower Development Program for Energy & Resources supported by the Ministry of Knowledge Economy (MKE), Korea.

References

[1] M. Takemoto, A. Chiba, H. Akagi and T. Fukao, “Radial force and torque of a bearingless switched reluctance motor operating in a region of magnetic saturation,” *in Conf. Record IEEE-IAS Annual Meeting*, pp. 35–42, 2002.

[2] M. Takemoto, K. Shimada, A. Chiba and T. Fukao, “A design and characteristics of switched reluctance type bearingless motors,” *in Proc. 4th Int. Symp. Magnetic Suspension Technology*, Vol. NASA/CP-1998-207654, pp. 49-63, May 1998.

[3] Li Chen, Wilfried Hofmann, “Analytically computing winding currents to generate torque and levitation force of a new bearingless switched reluctance motor,” *in Proc.12th EPE-PEMC*, pp. 1058-1063. Aug. 2006.

[4] Carlos R. Morrison. *Bearingless Switched Reluctance Motor. U.S.* Patent 6,727,618, 2004.

[5] C. S. Kim, M. G. Kim, H. G. Lee and J. W. Ahn, "Development of SRM and drive system for small pallet truck," *Annual Proc. of KIEE*, pp.732-734, 2000.

[6] C. S. Kim, S. G. Oh, J. W. Ahn and Y. M. Hwang, "The design and the characteristics of SRM drive for low speed vehicle," *Annual Proc. Of KIEE*, pp. 871-873, 2001.

[7] K. Ohyama, M. Naguib, F. Nashed, K. Aso, H. Fujii, H.

Uehara, "Design using finite element analysis of a switched reluctance motor for electric vehicle," *Journal of Power Electronics*, Vol. 6. No. 2, pp. 163-171, April 2006.

[8] S. Ayari, M. besbes, M. Lecrivain, and M. Gabsi, "Effectes of the air gap eccentricity on the SRM vibrations," *in Proc. Int. Conf. Electr. Mach. and Drives*, pp. 138-140, 1999.

[9] N.R. Garrigan, W. L. Soong, C. M. Stephens, A. Storacc and T. A. Lipo, "Radial force characteristics of a switched reluctance machine," *in Proc. IEEE IAS Annu. Meeting*, Vol. 4, pp. 2250-2258, 1999.

[10] I. Husain, A. Radun, and J. Nairus, "Unbalanced force calculation in switched reluctance machines," *IEEE Trans. Magn.*, Vol. 36, No. 1, pp. 330-338.

[11] A. V. Radum, "Design considerations for the switched reluctance motor," *IEEE Trans. Ind. Applicat.*, Vol. 31, pp. 1079-1087, Sep./Oct. 1995.

[12] Texas Instruments, *TMS320F243/F241/C242 DSP Controllers Reference Guide - System and Peripherals*, January 2000.

Huijun Wang was born in Zhuhai, China, in 1980. He received a B.S. degree in electrical engineering and automation from Shenyang University of Technology, Shenyang, China, in 2003, and a M.S. and Ph.D. in electrical and mechatronics engineering from Kyungsung University, Busan, Korea, in 2007, and 2009, respectively. His current research interests include advanced motor drive systems and the design of power converters.

Dong-Hee Lee was born in 1970 and received his B.S, M.S., and Ph. D in Electrical Engineering from Pusan National University, Busan, Korea, in 1996, 1998 and 2001, respectively. He worked as a Senior Researcher for the Servo R&D Team at OTIS-LG, from 2002 to 2005. He has been with Kyungsung University, Busan, Korea, as an assistant professor in the Department of Electrical and Mechatronics Engineering since 2005. He has been the director of the Advance Electric Machinery and Power Electronics Center since 2009. His current research interests are servo systems and electrical motor drives with power electronics.

Jin-Woo Ahn was born in Busan, Korea, in 1958. He received his B.S., M.S., and Ph.D. in Electrical Engineering from Pusan National University, Pusan, Korea, in 1984, 1986, and 1992, respectively. He has been with Kyungsung University, Busan, Korea, as a professor in the Department of Electrical and Mechatronics Engineering since 1992. He was a visiting researcher in the Speed Lab at Glasgow University, U.K., a visiting professor in the Dept. of ECE and WEMPEC at the University of Wisconsin-Madison, USA, and a visiting professor in the Dept. of ECE at Virginia Tech from July 2006-June 2007. He was the director of the Advance Electric Machinery and Power Electronics Center. He has also been the director of the Smart Mechatronics Advanced Research and Training Center since Aug. 2008 and the Senior Easy Life Regional Innovation System since July 2008, which are authorized by the Ministry of Knowledge Economy, Korea. He is the author of five books including SRM, the author of more than 100 papers and has several patents. His current research interests are advanced motor drive systems and electric vehicle drives. Dr. Ahn has received several awards including a Best Paper Award from the Korean Institute of Electrical Engineers in 2002 , the Korean Federation of Science and Technology Society in 2003, and the Korean Institute of Power Electronics in 2007, respectively. He is a senior member of the Korean Institute of Electrical Engineers, a member of the Korean Institute of Power Electronics and a senior member of the IEEE.